Portable Microcoil NMR Detection Coupled to Capillary Electrophoresis

ARTICLE *in* ANALYTICAL CHEMISTRY · FEBRUARY 2011

Impact Factor: 5.64 · DOI: 10.1021/ac102389b · Source: PubMed

7 AUTHORS, INCLUDING:

Kristl L Adams
Lawrence Livermore National Laboratory
15 PUBLICATIONS **72** CITATIONS
SEE PROFILE

Greg Klunder
Lawrence Livermore National Laboratory
29 PUBLICATIONS **238** CITATIONS
SEE PROFILE

Carla Vogt
Leibniz Universität Hannover
78 PUBLICATIONS **2,562** CITATIONS
SEE PROFILE

Julie Herberg
Lawrence Livermore National Laboratory
46 PUBLICATIONS **457** CITATIONS
SEE PROFILE

analytical chemistry

ARTICLE

pubs.acs.org/ac

Portable Microcoil NMR Detection Coupled to Capillary Electrophoresis

Joana Diekmann,[†] Kristl L. Adams,[‡] Gregory L. Klunder,[‡] Lee Evans,[‡] Paul Steele,[‡] Carla Vogt,[†] and Julie L. Herberg*[,‡]

[†]Department of Analytical Chemistry, Institute of Inorganic Chemistry, Faculty of Natural Sciences, Leibniz University Hanover, Callinstrasse 1, 30167 Hanover, Germany

[‡]Lawrence Livermore National Laboratory, 7000 East Avenue, Livermore, California 94550, United States

Supporting Information

ABSTRACT: High-efficiency separation techniques, such as capillary electrophoresis (CE), coupled to a nondestructive nuclear magnetic resonance (NMR) spectrometer offer the ability to separate, chemically identify, and provide structural information on analytes in small sample volumes. Previous CE−NMR coupled systems utilized laboratory-scale NMR magnets and spectrometers, which require very long separation capillaries. New technological developments in electronics have reduced the size of the NMR system, and small 1−2 T permanent magnets provide the possibilities of a truly portable NMR. The microcoils used in portable and laboratory-scale NMR may offer the advantage of improved mass sensitivity because the limit of detection (LOD) is proportional to the coil diameter. In this work, CE is coupled with a portable, briefcase-sized NMR system that incorporates a microcoil probe and a 1.8 T permanent magnet to measure ^{19}F NMR spectra. Separations of fluorinated molecules are demonstrated with stopped- and continuous-flow NMR detection. The results demonstrate that coupling CE to a portable NMR instrument is feasible and can provide a low-cost method to obtain structural information on microliter samples. An LOD of 31.8 nmol for perfluorotributylamine with a resolution of 4 ppm has been achieved with this system.

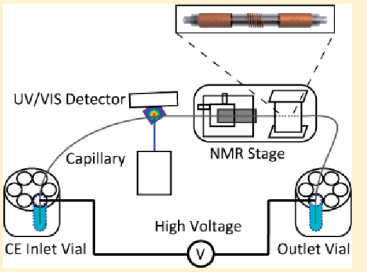

As investigations on pharmaceutical drugs and hazardous environmental samples are on the rise, the need for inexpensive, portable, and rapid chemical analysis tools for use in the pharmaceutical and medical-health industries as well as environmental field testing is increasing. These analytical problems many times involve 3D structure determinations of newly synthesized or environmental compounds, which are provided by nuclear magnetic resonance (NMR) instruments. However, laboratory-scale NMR instruments are large and expensive and have high continuing maintenance costs, thus making them infeasible for many environmental, pharmaceutical, and health industry laboratories to utilize extensively.

Portable liquid-state NMR[1−3] and NMR relaxometry[4] are rapidly growing research areas. In addition, separation techniques, such as liquid chromatography (LC) and capillary electrophoresis (CE), are being routinely coupled to laboratory-scale NMR spectrometers and now to portable NMR spectrometers to separate, identify, and provide structural information on analytes in small (nanoliter to microliter) sample volumes. More information can be gained with the possibility of adding multidimensional online detection in conjunction with portable CE−NMR including mass spectrometry (MS), laser-induced fluorescence (LIF), and ultraviolet/visible (UV/vis) spectroscopy. The use of capillary separation and detection methods minimizes the sample and solvent requirements, thus reducing the cost of each analysis. These advantages lead to the integration of CE into a portable NMR system having the potential to create unique analytical solutions for a wide range of industrial and technological scientific problems.

The first coupling experiments between NMR spectroscopy and CE were performed by Sweedler[5,6] and Albert[7,8] more than 15 years ago. This coupling relied on the development of a flow-through NMR probe to allow a sample to be directly introduced into the NMR microcavity after the compounds had been separated by CE, in both stopped-flow[9,10] and continuous-flow[10−12] modes. These developments took advantage of solenoid radio frequency (RF) microcoils with diameters of hundreds of micrometers to a few millimeters wound directly around the separation capillary, providing a high filling factor,[13] which improved the sensitivity of the NMR signal.[14] Due to stronger coupling to the sample, solenoid coils are about twice as sensitive as saddle coils, which are typically used in traditional liquid-state NMR analysis and are necessary for vertically inserted samples.[15] Furthermore, reducing the active coil size and the sample volume, while leaving the sample mass constant, improves the mass sensitivity[16] (see eqs 1 and 2). Hoult and Richards[15] developed a mathematical equation describing this relationship between the RF coil diameter and the NMR sensitivity; in addition, Peck et al.[17] also demonstrated experimentally that this relationship is accurate for microcoils with a diameter smaller than 100 μm. The mathematical

Received: September 27, 2010
Accepted: December 13, 2010
Published: January 14, 2011

correlation shows that the signal-to-noise ratio (SNR) is inversely proportional to the diameter of the receiver coil (see eq 1). Since RF coils with smaller diameters are limited in the detectable volume, microcoil NMR is truly beneficial when working with concentrated, mass-limited samples, as may be commonly encountered in pharmaceutical analysis. To obtain a maximum mass sensitivity, the sample needs to be measured in the smallest RF coil diameter which includes the total sample volume.[18,19]

In addition, CE can increase the sensitivity of NMR by online preconcentration[20] of the sample using a simple electrokinetic injection or through other stacking techniques such as isotachophoresis (ITP),[21−23] electrokinetic focusing, or counterflow CE.[24]

Recent advancements in permanent magnets and electronics have led to the miniaturization of the entire NMR system. Previous works describing couplings of CE to NMR were all performed on laboratory-scale NMR systems that cannot be used outside the laboratory. The recent development of portable liquid-state NMR systems can be attributed to the working groups around Demas,[1] McDowell,[3] and Danieli.[2] Due to the small size of the RF coil, the power required for the nuclear excitation is also lower; thus, smaller RF amplifiers can be used.[1] In addition, SmCo magnets can generate adequate magnetic field strengths of 0.2−2.0 T with a size of less than 10 cm × 5 cm, weighing less than 700 g. Demas et al.[1] utilizing a laser lithographic coil design demonstrated resolutions in the parts per million range for ^{19}F NMR spectra with a 1.8 T magnet. McDowell et al.[3] published results achieving resolutions in the sub parts per million range for ^{1}H NMR spectra with a 1 T magnet and an auxiliary inductor circuit. Danieli et al.[2] also reported a sub parts per million resolution using standard 5 mm NMR sample tubes and a 0.7 T Halbach magnet weighing less than 500 g and designed specifically to homogenize the magnetic field. These approaches show that NMR detectors with low-field permanent magnets can be operated in a new size and frequency regime.

The targeted area of application for the research being presented in this paper concerns fluorinated compounds. The analysis of these fluorinated substances is of great interest, as more and more fluorinated compounds are used in the synthesis and purification of pharmaceuticals,[25] as well as in artificial blood substitutes[26] and in everyday products, e.g., Gore-Tex[27] or Teflon.[28] Furthermore, trifluoroacetic acid (TFA) and longer chain perfluorinated carboxylic acids (PFCAs) are degradation products of atmospheric pollutants such as chlorofluorocarbons and hydrofluorocarbons.[29,30] All of these perfluorinated products are ubiquitous in the environment and often found in humans and biota. Their persistent properties lead to bioaccumulation and have shown potential toxicity effects.[31,32] Therefore, it is important to develop efficient and reliable analytical methods for the determination of the fluorinated components in the environment and in the products intended for human use.[33]

Separation and analytical determination of fluorinated compounds have been demonstrated by a variety of analytical techniques, such as gas chromatography,[34−36] MS,[37,38] ^{19}F NMR,[39,40] CE,[41] and other chromatographic methods.[42−45] The advantage of using CE and ^{19}F NMR for the direct analysis of fluorinated compounds is that no derivatization is needed and the whole structure can be identified in one experiment.[31] For this reason, both ^{19}F NMR and CE are already widely used for the study of fluorinated compounds in various matrixes.[46−48] Therefore, it is desirable to have online coupling of these two methods, where CE provides a highly efficient separation and concentration method and coupled NMR offers a nondestructive, structure-elucidating detection technique.

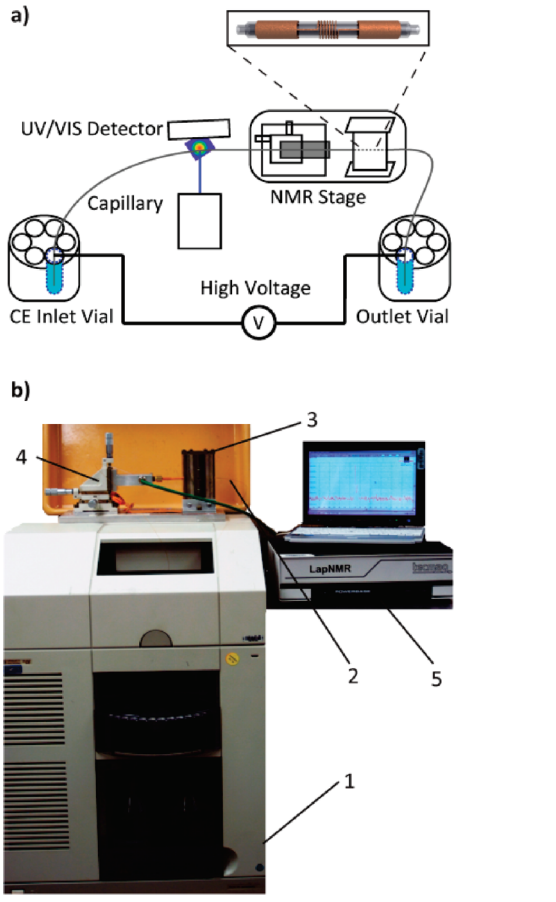

Figure 1. (a) Schematic diagram of the CE−NMR system. Close-up: capillary-in-capillary configuration for the CE−NMR analysis. (b) Picture of the CE (1) and separation capillary (2) coupled to the portable microcoil NMR system with a 1.8 T magnet (3), a home-built probe with a translation stage for its positioning (4), and a spectrometer (5).

The current work emphasizes the first attempt of coupling CE with a portable microcoil NMR system using a capillary-in-capillary construction (see Figure 1a) with the ^{19}F NMR RF microcoil. This capillary configuration has the advantage of using the laser-lithographic[50] or hand-wound microcoils on the outer capillary with the inner capillary for separations. Thus, the separation capillary can be easily changed to accommodate different separation conditions, e.g., coated capillaries, or replacing them when clogged or broken. We are reporting on resolution and sensitivity measurements performed with TFA and perfluoropentanoic acid (PFPA) using this portable NMR design coupled to CE.

EXPERIMENTAL SECTION

Reagents and Chemicals. Analytical grade sodium hydroxide was used for capillary conditioning (Fluka, Buchs, Switzerland). Perfluorotributylamine (FC-43, $C_{12}F_{27}N$) (3M, Saint Paul, MN, U.S.) was used for limit of detection (LOD) measurements and as a reference compound in the portable NMR system (see the Supporting Information, Table S-1). Ultrapure water from an in-house Milli-Q purification (Eschborn, Germany) system and analytical grade chemicals (TFA, PFPA, difluoroacetic acid (DFA), *o*-phthalic acid, and hexadecyltrimethylammonium

bromide (HTAB)) were used for the preparation of all buffers and samples.

CE System. An automated HP^{3D}CE (Agilent Technologies, Santa Clara, CA, U.S.) capillary electrophoresis unit equipped with a photodiode-array UV/vis detector (190−600 nm), automatic pressure or electrokinetic sample injection, an autosampler, an air-cooled capillary cartridge, and a 30 kV high-voltage supply was used. The 3D-CE ChemStation software (revision A.10.02) was used for system control, data collection, and data analysis. The uncoated fused silica capillaries (Polymicro Technologies Inc., Phoenix, AZ, U.S.) had a 50 μm i.d. (360 μm o.d.) and a 5 mm long detection window at 50 cm (total length 58.5 cm). The separation electrolyte consisted of 5 mM *o*-phthalic acid (pK_{a1} = 2.9 and pK_{a2} = 5.5), and HTAB was added with a concentration of 0.27 mM, resulting in a pH of 5.3. The capillary was conditioned with 1.0 M NaOH for 30 min and 0.1 M NaOH for 15 min, followed by a 30 min rinse with the separation buffer (special rinsing vial). The sample injection followed at 40 mbar (4 kPa) for 4 s, the separation took place at a voltage of 20 kV under negative polarity at 25 °C, and the indirect detection was monitored at 214 nm.

Portable NMR System. The portable microcoil NMR instrument was a home-built system developed at the Lawrence Livermore National Laboratory (see Figure 1a) and included a compact spectrometer, hand-held permanent magnet, microprobe with hand-wound microcoil, power amplifier (SpinCore Technologies, Inc., Gainesville, FL, U.S.), and laptop computer.[1] The spectrometer was commercially available (LapNMR, Tecmag Inc., Houston, TX, U.S.) and connected to a laptop computer for instrument control and data processing with the supplied software (NTNMR, Tecmag Inc.). The permanent magnet was a 1.8 T SmCo box magnet (Aster Enterprise, Inc., Acton, MA, U.S.) with excellent shielding properties, important for a portable system and a uniform magnetic field in the center of the box magnet.[49] The microcoil for the following experiments was hand-wound onto a short length of capillary and had 30 turns, a length of 1740 μm, and a 410 μm i.d. (454 μm o.d.). Each sample was measured using a one-pulse NMR analysis at a ^{19}F coupled frequency of 71.880−71.968 MHz.

CE−NMR System. For the integration of the portable NMR with the CE system (see Figure 1b) a 1.5 m long, 200 μm i.d. (300 μm o.d.) fused silica CE capillary was inserted through the microprobe in the NMR stage to enable online detection. The observable NMR volume was 55 nL. Two acquisition modes (stopped and continuous flow) and two injection techniques (hydrodynamic and electrokinetic) were used for the CE−NMR experiments. The CE capillary was inserted into the capillary which had the RF microcoil wound onto it (see close-up representative schematic Figure 1a).

RESULTS AND DISCUSSION

Coupling CE and NMR. On the basis of the CE separation methods presented by Hettiarachchi et al.[48] and Little et al.,[41] a buffer matrix with 5 mM *o*-phthalic acid and 0.27 mM HTAB (pH 5.3) was used for the separation of the three fluorinated substances DFA, TFA, and PFPA. This buffer and the reversed polarity conditions yielded the best results, separating the compounds with reproducible and Gaussian-shaped peaks using a 50 μm i.d. capillary. Other separation parameters were implemented during the coupling of CE and NMR as indicated in each section below.

Coupling of CE with portable online NMR detection can be a balancing act between the optimum operating conditions for each technique. Although the RF microcoil improves the NMR sensitivity, the concentrations required are still relatively high for adequate CE resolution and can result in overlapping peaks. In this work, nonstandard CE conditions were incorporated by using 200 μm i.d. capillaries to increase the amount of analyte in the NMR detection window, which also leads to poor peak resolution, discussed below. In addition, the voltage applied during the CE separation can have adverse affects on the NMR signal. Sweedler et al.[14] and Webb[18] demonstrated how a second local magnetic field induced by the electrophoretic current in the CE capillary distorts the magnetic field homogeneity produced by the RF coil. This effect of induced magnetic fields causes line broadening and poor SNR in the NMR signals. To eliminate this effect, the voltage was turned off during NMR data acquisition and the experiments were performed in a stopped-flow mode with mobilization via pressure or voltage.

In the stopped-flow experiments, the voltage was turned off for a specific period of time when the analyte reached the NMR microcoil to allow for repeated NMR scans. Diffusion effects were of concern during the stopping of the CE voltage, particularly due to the larger capillary i.d. (200 μm) used for the separations. These diffusion effects were investigated by hydrodynamically injecting a TFA sample and allowing the sample plug to remain in the capillary for defined periods of time before UV/vis analysis. After the sample injection, the voltage was switched off after 2 min, shortly before the TFA would reach the UV/vis detector window. The run was then paused for different periods of times (0, 1, and 5 min) before the sample was forced past the detection window and out of the capillary with a pressure of 50 mbar (5 kPa). Two characteristics were observed and are presented in Figure 2a. First, the applied pressure mobilizes the sample at a slower velocity than the separation voltage, which causes an increased peak width for the pressure runs as compared to the voltage-only run (blue trace). Second, the peak migration time of the 1 min (green trace) and 5 min (purple trace) runs directly reflects the stop time as compared to the stop voltage, immediately apply pressure (0 min, red trace) run. These results show that using pressure can be beneficial due to the slower sample movement through the capillary, which could enable more NMR scans to be acquired with a continuous-pressure-flow mode. Furthermore, no significant diffusional broadening was observed for the different stop times on the basis of the peak widths. Peak heights may provide better evidence of peak diffusion effects because the height correlates with the concentration; therefore, individual peak heights were compared to each other. The peak heights of the 0, 1, and 5 min runs varied by less than 3%; thus, diffusion effects were determined to be minimal during stopped-flow operation and should not be of concern. Accordingly, diffusional effects are not expected to have a significant influence on the results when longer NMR acquisition times are required.

As an alternative to applying pressure to move the sample into the NMR coil, voltage can be used to precisely position the sample by alternately switching the positive and negative polarities. Figure 2b shows an electropherogram of the separation of a DFA-doped TFA solution (2.85 mM) with switching polarities (20 kV) to position the sample in the capillary. The DFA was used in a low concentration (0.3 mM) to visualize the changing flow directions of the sample (initially with negative voltage the large TFA peak is followed by the small DFA spike). At 3.2 min

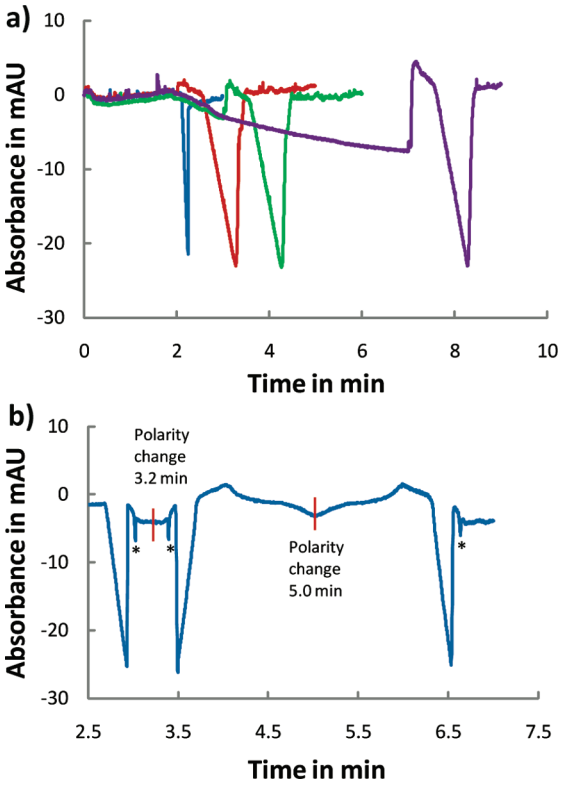

Figure 2. Electropherograms of a 2.85 mM TFA sample (a) using voltage for the whole run (blue trace) and voltage for 2 min and stopping the run for different amounts of time, before the sample is pushed out with 50 mbar of pressure (stopping for 0 min (red trace), 1 min (green trace), and 5 min (purple trace)). In (b) the TFA sample was doped with 0.5 mM DFA (* peaks); alternating voltage polarity switching (20 kV, 4 s injection with 40 mbar) is indicated by red bars.

the voltage polarity was switched to positive so that the analytes were migrating in the reverse direction (DFA spike followed by large TFA peak). The TFA sample first passed the detector window at about 2.9 min and a second time at 3.5 min. When the voltage polarity was switched yet again at 5 min, the analyte passed the detector for a third time as seen by the large TFA peak at 6.5 min again followed by the small DFA spike. Detection times showed that the changing points of the polarity are always in the mirrored peak pattern, as would be expected, and thus provided an accurate method to manipulate plug positioning. Furthermore, no diffusional peak broadening was detected, and the peak heights and peak widths varied by less than 2% and 5%, respectively. These results show that using voltage for the sample positioning was more controllable and accurate than using pressure, since alternating voltage does not produce the velocity changes seen under the pressure conditions. Thus, UV/vis absorption data suggest using either pressure mobilization or electrophoretic positioning should not detrimentally affect the width of the sample plug.

Another consideration in addressing the balancing act between CE and NMR is providing enough sample for the microcoil NMR detection, while still achieving complete chemical separation via CE. An important necessity for high NMR sensitivity is maximizing the filling factor or increasing the sample volume inside the NMR observable coil volume to maximize detectable nucleus spins. For normal CE separations, capillary i.d.'s of 50−100 μm are typically used. However, in this work, capillaries with a 200 μm i.d. were used to provide a greater coil filling factor to increase the NMR sensitivity at the expense of a loss in CE separation resolution due to Joule heating effects. Using even larger i.d. separation capillaries, especially in the region of the NMR coil window such as with bubble-cell capillaries would be desirable to increase the coil filling factor more and thus increase the LOD. However, the capillary-in-capillary design has the technical limitation of only allowing a fixed OD separation capillary (300 μm o.d. in this case) to fit through the outer microcoil capillary. The capillary-in-capillary design has a reduced coil filling factor; however, the convenience of easily exchanging the CE separation capillary is a great advantage of this design.

In addition to increasing the capillary i.d., another consideration for improving the NMR LOD is to provide high sample concentrations (c), which can be detected by the portable NMR spectrometer within a short acquisition time frame (t_{acq}). Microcoils with a smaller diameter (d_{coil}) and coil height (h) have a higher mass sensitivity than larger RF coils used for conventional liquid-state NMR analysis. To take advantage of the increased SNR offered by the smaller RF coil, there must be means by which the mass of the sample (the total number of spins) can be introduced into the smaller volume of the microcoil, so that the number of resonant nuclei are held constant. This means the sample concentration must increase as the resonant coil volume (V) decreases, to maintain the mass sensitivity, as stated in the following equations:[15,17]

$$\mathrm{SNR} = \frac{\text{peak signal}}{\text{root mean square noise}} \propto \frac{V\left(d_{coil}\sqrt{1+(h/d_{coil})^2}\right)^{-1}}{\text{RMS noise}} \quad (1)$$

$$\mathrm{LOD} = \frac{3c\sqrt{t_{acq}}}{\mathrm{SNR}} \quad (2)$$

While online CE−NMR analysis offers several advantages including online chemical separation, concentration, and speciation as well as complementary sample analysis, some concessions must be made, specifically involving the sample concentration. A significant discrepancy exists between the concentrations (typically 10−1000 mM) required to obtain sufficient SNR in portable NMR using microcoil detectors in lower field, lower resolution magnets such as those described in this paper and the concentrations (typically 0.1−10 mM) used in CE analysis. One of the challenges of working at high concentrations involves ambiguity in the interpretation of optical UV/vis data. This is especially pronounced when the sample has a small absorptivity at the detection wavelength. For example, as seen in Figure 3a, a 3.56 M TFA sample plug was pushed through the capillary using 30 mbar (3 kPa) of pressure, and unexpected peak shapes were acquired at different UV/vis wavelengths. At longer wavelengths (254 and 280 nm) the TFA signal resulted in the expected single negative peak. However, at 214 nm, which is the normal detection wavelength for this separation, a double peak was observed. Total absorbance is directly proportional to the concentration of the absorbing species in the solution as stated by the Beer−Lambert law.[51] The pure TFA absorption spectrum (not shown) measured in a capillary reached a maximum molar absorptivity at 420 dm^2 mol^{-1} in the low-wavelength range (190−220 nm) and then gradually decreased to a molar absorptivity of

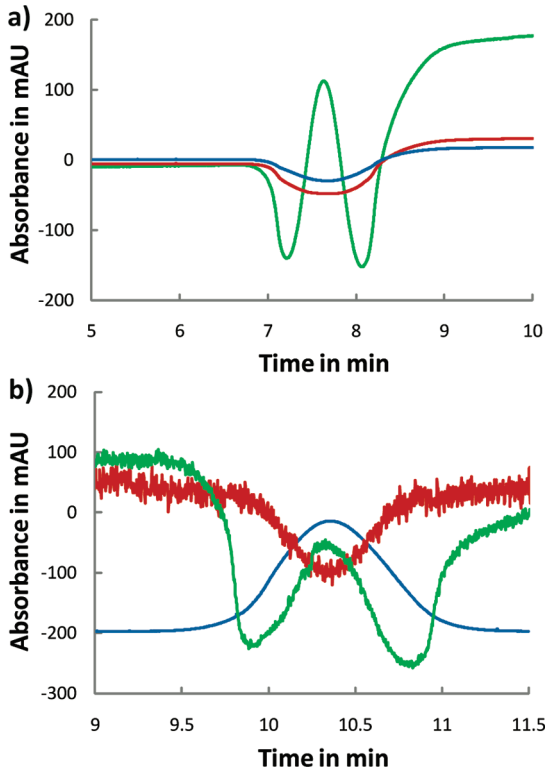

Figure 3. A 3.56 M TFA sample using a 5 mM phthalic acid buffer as BGE, a 30 mbar pressure run, and 4 s injection with 40 mbar: (a) electropherograms of the TFA peak at different wavelengths (green trace, 214 nm; red trace, 254 nm; blue trace, 280 nm), (b) reconstruction of the same double peak represented in (a) using different experiments, 0.65 M TFA dissolved in water (blue trace), 0.66 M TFA dissolved in BGE (red trace), and 3.56 M TFA dissolved in BGE (green trace).

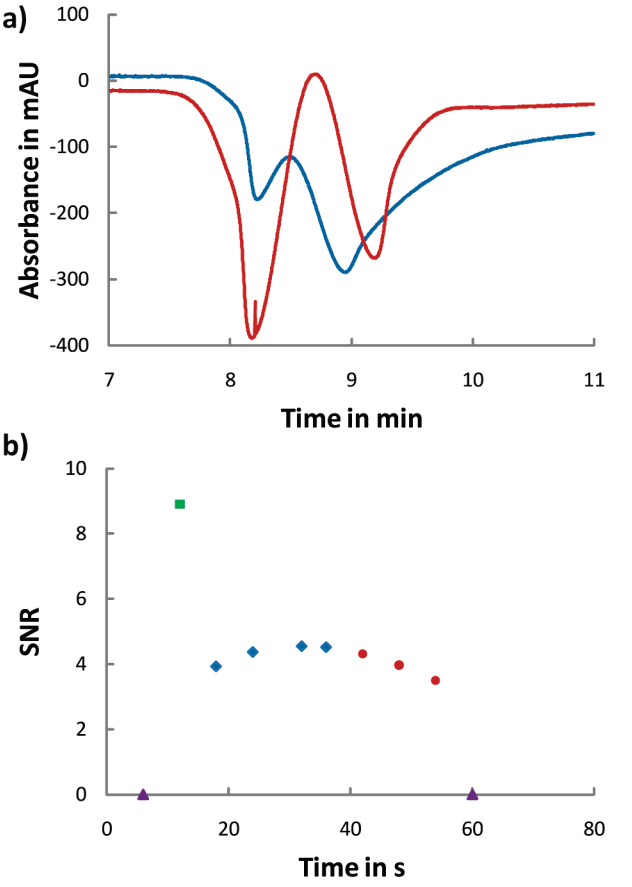

Figure 4. (a) Electropherogram of 1.8 M TFA and 0.6 M PFPA with negative electrokinetic injection (30 kV and 30 s) using 5 mM phthalic acid, pH 5.3, and a 30 mbar pressure run (blue trace) and a combined voltage−pressure run (red trace) in a 200 μm i.d. capillary, 150 cm long. (b) SNR of ^{19}F NMR spectra (32 scans, 8.2 μs pulse width) of TFA (green square), PFPA (red circles), and a TFA−PFPA mixture (blue tilted squares) plotted versus the monitored time in seconds. The purple triangles represent the NMR spectra directly before and after the sample.

0.01 dm^2 mol^{-1} above 220 nm. The electropherograms in Figure 3a demonstrate how the TFA absorption at shorter wavelengths can result in double peaks which appear to be an overlapping of two different Gaussian peaks, one having a negative absorption and one positive compared to the background electrolyte (BGE). To demonstrate this, Figure 3b shows the TFA−water absorbance differences resulting in a positive peak for the TFA, whereas TFA−BGE resulted in a negative TFA peak. Thus, the double peak absorbance was the sum of those different absorbance coefficients as shown by the green trace in Figure 3b, which was produced by adding together the electropherograms of TFA−water (blue trace) and BGE−water (red trace). Although UV/vis indirect detection is most sensitive at 214 nm with this buffer system, at higher concentrations it could cause confusion, which would not be observed with NMR detection. These challenging high concentration parameters reinforce the continued need for higher NMR resolution to provide higher SNR so that the concentration gaps between the CE and NMR experiments can be narrowed.

Stopped-Flow and Continuous-Flow NMR. To obtain NMR spectra, the CE separation voltage should be off during the NMR data acquisition to prevent line broadening. In this section, the results from two methods, stopped- and continuous-flow separation modes with pressure mobilization, are presented. To demonstrate the stopped-flow method, a solution of 1.8 M TFA and 0.6 M PFPA was electrokinetically injected (30 kV for 30 s) into the 150 cm long separation capillary. In Figure 4a, the blue UV/vis trace results from a continuous 30 mbar pressure mobilization to move the analytes which were partially separated during the electrokinetic injection through the remainder of the capillary. The use of pressure results in longer experiment times. However, it is more convenient to use pressure when dealing with highly concentrated solutions and large i.d. capillaries, because excess Joule heating would be created by the large amount of current running through the capillary. A better separation of the sample was achieved by applying a 15 kV voltage for 1.5 min after injection and concurrent with the continuous 30 mbar pressure lasting until the sample exits the capillary. The voltage was applied in the opposite direction of the capillary pressure flow, so that the peaks stack together and separate (see Figure 4a, red trace). The combined pressure−voltage experiment shows marked CE separation improvement over the pressure-only run with almost baseline separation and improved sample concentration.

In the following experiment, the above-described combined pressure−voltage method is used for online NMR data acquisition of the TFA and PFPA samples. The CE method is stopped periodically to allow NMR scans of the traversing sample plugs. In the resulting NMR spectra (not shown), the SNR values and the peak shapes of the individual signals were used to identify the

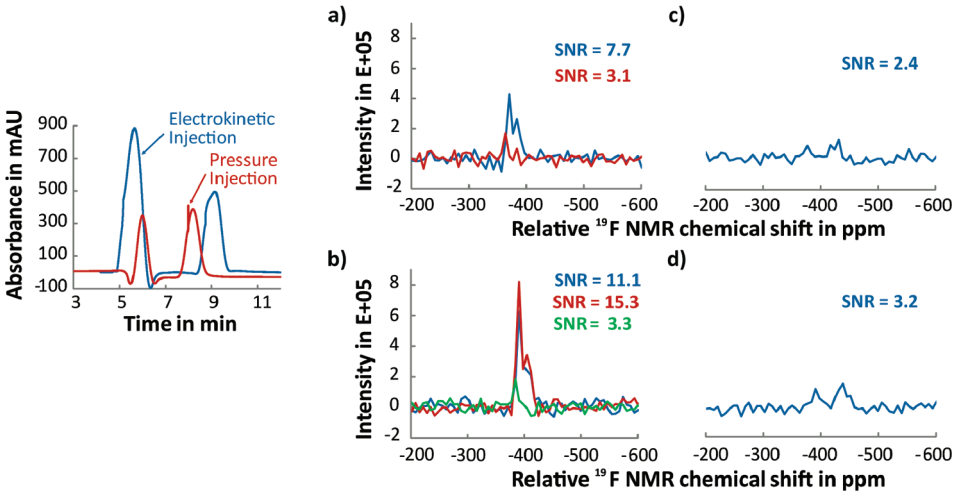

Figure 5. Left: Electropherogram of 6.74 M TFA and 1.15 M PFPA with 5 mM phthalic acid, pH 5.3, during a 30 mbar pressure run (200 μm i.d. capillary, 150 cm long) using individual pressure and electrokinetic injections. Right: ^{19}F NMR spectra of TFA and PFPA acquired during the continuous-flow run (32 scans, 8.2 μs pulse width) with (a) pressure injection (40 mbar for 4 s) for TFA, (b) voltage injection (15 kV for 240 s) for TFA, (c) pressure injection (40 mbar for 4 s) for PFPA, and (d) voltage injection (15 kV for 240 s) for PFPA. Different colors represent consecutive NMR scans in time, in the order of blue peak, red peak, and green peak.

two separated substances in the spectrum. This proof of concept experiment necessitated a prior knowledge of NMR spectra, such as the location of peaks and the number of scans required for sufficient SNR to observe the peaks. In Figure 4b, the SNRs for the NMR peaks are plotted against the migration time. The colors in the spectrum represent the two different substances, TFA as a green square and PFPA as red circles, and blue tilted squares represent the mixture of PFPA and TFA, indicating that the analytes were not yet completely separated. This incomplete sample separation is verified in the UV/vis CE electropherogram in Figure 4a. The overlapping peaks may be due to plug diffusion during repeated stopped flow and pressure mobilization. Reference spectra (see the Supporting Information, Figure S-1) of the individual compounds, TFA and PFPA, were acquired for comparison to the spectra obtained during the online pressure—voltage stopped-flow separation of the sample mixture. The TFA sample had a high singlet peak in the online spectrum with an SNR of 9 which was initially resolved then for the next 20 s; a mixture of PFPA and TFA was detected. At the end of the stopped-flow acquisition, the pure PFPA substance was detected, resulting in two NMR peaks with a peak height ratio of 3:6, matching the reference structure of PFPA. These preliminary results show that qualitative results obtained with the UV/vis and NMR detection are consistent (see the Supporting Information, Figure S-2).

Ideally, NMR detection would be achieved in a continuous-flow mode so that precise positioning of the sample in the detection window is not required. Separations were achieved with the voltage applied at the beginning for 1.5 min, and then the sample was mobilized to the NMR detector by applying a constant pressure (50 mbar). Since the pressure flow is considerably slower than the electrokinetic flow, there is adequate time for NMR analysis. Figure 5 shows these results using two different injection modes, electrokinetic and hydrodynamic. The electrokinetic method shows an on-column CE preconcentration effect and biased sample injection as seen in the electropherograms (see Figure 5, left panel) by the significant difference in the peak areas and heights of the two peaks. The UV/vis peak of TFA, which was the fastest migrating substance, had a 2.3 times larger area when using the electrokinetic injection. In comparison to the TFA peak, the PFPA peak showed a 1.5-fold increased peak area, indicating that the electrokinetic injection preferentially preconcentrates the highly charged, smaller, and more mobile TFA molecule compared to the larger, less mobile PFPA molecule, which is consistent with the theoretical assumptions. Online NMR spectra were acquired for both continuous-flow CE separations shown. The ^{19}F NMR spectra demonstrate that pure TFA and PFPA signals can be acquired with this method (see Figure 5, right panel). The different colors in these TFA and PFPA plots represent NMR scans in time (blue peak, red peak, and green peak consecutively) and show plug movement through the NMR coil. The electrokinetic preconcentration results seen in the UV/vis electropherogram are reflected in the NMR SNR values, whereas pressure injection shows lower SNR values than the electrokinetic injection seen in Figure 5 (right panel). The SNR values of the TFA were approximately 2 times higher for the electrokinetic injection than those for the pressure injection, and for the PFPA the difference was about 1.3-fold. These results demonstrate that both CE and NMR give the same qualitative and quantitative results using a continuous-flow or stopped-flow pressure-mobilized experiment.

CONCLUSIONS

This is the first demonstration of a coupled microseparation technique to a miniaturized information-rich NMR detection system, which offers a cost-effective system to obtain structural information about samples of interest from the pharmaceutical and environmental fields. The results of this new attempt to couple CE with portable microcoil NMR confirm that it is possible to do online measurements using a capillary-in-capillary configuration, though under severe CE separation conditions. In these proof-of-concept experiments we were able to extract structural information from the NMR spectra and comparable, online semiquantitative data with the CE UV/vis electropherogram and the ^{19}F NMR spectra. Further developments in higher magnet resolution and higher magnetic field strength as well as improved RF sensitivity will benefit CE separations and NMR structural

elucidations by lowering the required sample concentrations. In the near future higher magnet resolution is conceivable, with the addition of shim coils, to provide the greatest resolution enhancement.

However, there are still a number of challenges which exist and require further research and development. To improve the CE−NMR data acquisition and separation, it would be desirable to have a setup which allows the CE to have a continuous voltage separation during NMR spectral acquisition. Hergenröder et al.[52] demonstrated the coupling of CE with NMR using a microstrip NMR coil, allowing continuous voltage NMR data acquisition, because the microstrip creates a magnetic field perpendicular to the $\mathbf{B}_0$ field. Thus, the microstrip does not lead to inhomogeneity within the sample space, unlike the current solenoid coil. However, implementing this new slotted coil setup into the portable NMR system entails the use of a new permanent magnet design, currently in development. An alternative approach to improve the CE resolution is to normalize the CE separation conditions by using smaller i.d. capillaries and etching a bubble cell which widens the i.d. of the capillary in the region of the NMR coil window. This capillary design has the effect of converting a long, narrow CE band into a shorter, wider band which would fill the bubble cell sufficiently, so that more nucleus spins are in the active NMR coil volume. By widening the inner diameter of the CE capillary in the NMR coil window, an increased sample volume of approximately 25-fold (from 50 to 250 μm) can be attained in the active coil detection volume. In addition, further sample preconcentration techniques, such as ITP, are desirable to have even higher substance concentrations in the NMR microcoil. A further advantage for the coupled CE−portable NMR system would be the introduction of a portable CE instrument offering a reduced footprint and portability of these combined analytical techniques.

The here demonstrated studies of this unique online-coupled CE−NMR system form an initial foundation for future analytical research into portable CE−NMR coupled systems.

■ ASSOCIATED CONTENT

Supporting Information. Additional information as described in the text. This material is available free of charge via the Internet at http://pubs.acs.org.

■ AUTHOR INFORMATION

Corresponding Author
*Phone: (925) 422-5900. E-mail: herberg1@llnl.gov.

■ ACKNOWLEDGMENT

This work was supported and performed under the auspices of the U.S. Department of Energy by Lawrence Livermore National Laboratory under Contract DE-AC52-07NA27344.

■ REFERENCES

(1) Demas, V.; Herberg, J. L.; Malba, V.; Bernhardt, A.; Evans, L.; Harvey, C.; Chinn, S. C.; Maxwell, R. S.; Reimer, J. *J. Magn. Reson.* **2007**, *189*, 121–129.
(2) Danieli, E.; Perlo, J.; Blümich, B.; Casanova, F. *Angew. Chem., Int. Ed.* **2010**, *49*, 4133–4135.
(3) McDowell, A.; Fukushima, E. *Appl. Magn. Reson.* **2008**, *35*, 185–195.
(4) Eidmann, G.; Savelsberg, R.; Blümler, P.; Blümich, B. *J. Magn. Reson., A* **1996**, *122*, 104–109.
(5) Wu, N.; Peck, T. L.; Webb, A. G.; Magin, R. L.; Sweedler, J. V. *J. Am. Chem. Soc.* **1994**, *116*, 7929–7930.
(6) Wu, N.; Peck, T. L.; Webb, A. G.; Magin, R. L.; Sweedler, J. V. *Anal. Chem.* **1994**, *66*, 3849–3857.
(7) Albert, K.; Schlotterbeck, G.; Tseng, L. H.; Braumann, U. *J. Chromatogr., A* **1996**, *750*, 303–309.
(8) Albert, K. *Analysis* **1996**, *24*, M17–M18.
(9) Olson, D. L.; Lacey, M. E.; Webb, A. G.; Sweedler, J. V. *Anal. Chem.* **1999**, *71*, 3070–3076.
(10) Schewitz, J.; Pusecker, K.; Gfroerer, R.; Goetz, U.; Tseng, L.-H.; Albert, K.; Bayer, E. *J. Chromatogr.* **1999**, *50*, 333–337.
(11) Wolters, A. M.; Jayawickrama, D. A.; Webb, A. G.; Sweedler, J. V. *Anal. Chem.* **2002**, *74*, 5550–5555.
(12) Jayawickrama, D. A.; Sweedler, J. V. *Anal. Chem.* **2004**, *76*, 4894–4900.
(13) Lacey, M. E.; Subramanian, R.; Olson, D. L.; Webb, A. G.; Sweedler, J. V. *Chem. Rev.* **1999**, *99*, 3133–3152.
(14) Jayawickrama, D. A.; Sweedler, J. V. *J. Chromatogr., A* **2003**, *1000*, 819–840.
(15) Hoult, D. I.; Richards, R. E. *J. Magn. Reson.* **1976**, *24*, 71–85.
(16) Olson, D. L.; Norcross, J. A.; O'Neil-Johnson, M.; Molitor, P. F.; Detlefsen, D. J.; Wilson, A. G.; Peck, T. L. *Anal. Chem.* **2004**, *76*, 2966–2974.
(17) Peck, T. L.; Magin, R. L.; Lauterbur, P. C. *J. Magn. Reson.* **1995**, *108*, 114–124.
(18) Webb, A. G. *Magn. Reson. Chem.* **2005**, *43*, 688–696.
(19) Webb, A. G. *J. Pharm. Biomed. Anal.* **2005**, *38*, 892–903.
(20) Burgi, D. S.; Chien, R. L. *Anal. Chem.* **1991**, *63*, 2042–2047.
(21) Jung, B.; Bharadwaj, R.; Santiago, J. G. *Anal. Chem.* **2006**, *78*, 2319–2327.
(22) Korir, A. K.; Almeida, V.; Malkin, D. S.; Larive, C. K. *J. Am. Chem. Soc.* **2005**, *229*, U108–U108.
(23) Wolters, A. M.; Jayawickrama, D. A.; Sweedler, J. V. *J. Nat. Prod.* **2005**, *68*, 162–167.
(24) Meighan, M. M.; Staton, S. J. R.; Hayes, M. A. *Electrophoresis* **2009**, *30*, 852–865.
(25) Bégué, J.-P.; Bonnet-Delpon, D. *J. Fluorine Chem.* **2006**, *127*, 992–1012.
(26) Wakefield, B. *Innovations Pharm. Technol.* **2000**, 74–78.
(27) Gore, W. L. & Associates, Inc. *Die PTFE-Story*; Newark, DE, 2009.
(28) DuPont-Teflon. *How Are Teflon® Non-Stick Coatings Made*; Wilmington, DE, 2009.
(29) Berends, A. G.; Boutonnet, J. C.; de Rooij, C. G.; Thompson, R. S. *Environ. Toxicol. Chem.* **1999**, *18*, 1053–1059.
(30) Wallington, T. J.; Nielsen, O. J. *Organofluorine, The Handbook of Environmental Chemistry*; Springer: Berlin, 2002; Vol. 3, Part N.
(31) Ellis, D. A.; Moody, C. A.; Mabury, S. A. *Organofluorine, The Handbook of Environmental Chemistry*; Springer: Berlin, 2002; Vol. 3, Part N.
(32) Ritter, S. K. *Chem. Eng. News* **2010**, 88.
(33) Boutonnet, J. C.; Bingham, P.; Calamari, D.; de Rooij, C.; Franklin, J.; Kawano, T.; Libre, J. M.; McCulloch, A.; Malinverno, G.; Odom, J. M.; Rusch, G. M.; Smythe, K.; Sobolev, I.; Thompson, R.; Tiedje, J. M. *Hum. Ecol. Risk Assess.* **1999**, *5*, 59–124.
(34) Cahill, T. M.; Benesch, J. A.; Gustin, M. S.; Zimmerman, E. J.; Seiber, J. N. *Anal. Chem.* **1999**, *71*, 4465–4471.
(35) Cahill, T. M.; Seiber, J. N. *Environ. Sci. Technol.* **2000**, *34*, 2909–2912.
(36) Cahill, T. M.; Thomas, C. M.; Schwarzbach, S. E.; Seiber, J. N. *Environ. Sci. Technol.* **2001**, *35*, 820–825.
(37) Scott, B. F.; Alaee, M. *Water Qual. Res. J. Can.* **1998**, *33*, 279–293.
(38) Römpp, A.; Klemm, O.; Fricke, W.; Frank, H. *Environ. Sci. Technol.* **2001**, *35*, 1294–1298.
(39) Zuber, G. E.; Staiger, D. B.; Warren, R. J. *Anal. Chem.* **1983**, *55*, 64–67.

(40) Ellis, D. A.; Martin, J. W.; Muir, D. C. G.; Mabury, S. A. *Anal. Chem.* **2000**, *72*, 726–731.
(41) Little, M. J.; Aubry, N.; Beaudoin, M. E.; Goudreau, N.; LaPlante, S. R. *J. Pharm. Biomed. Anal.* **2007**, *43*, 1324–1330.
(42) Fernando, P. N.; McLean, M. A.; Egwu, I. N.; deGuzman, E.; Weyker, C. *J. Chromatogr., A* **2001**, *920*, 155–162.
(43) Kaiser, E.; Rohrer, J. *J. Chromatogr., A* **2004**, *1039*, 113–117.
(44) Standley, L. J.; Bott, T. L. *Environ. Sci. Technol.* **1998**, *32*, 469–475.
(45) Wiegand, C.; Pflugmacher, S.; Giese, M.; Frank, H.; Steinberg, C. *Ecotoxicol. Environ. Saf.* **2000**, *45*, 122–131.
(46) Monte, S. Y.; Ismail, I.; Mallett, D. N.; Matthews, C.; Tanner, R. J. N. *J. Pharm. Biomed. Anal.* **1994**, *12*, 1489–1493.
(47) Preiss, A.; Kruppa, J.; Buschmann, J.; Mügge, C. *J. Pharm. Biomed. Anal.* **1998**, *16*, 1381–1385.
(48) Hettiarachchi, K.; Ridge, S. *J. Chromatogr., A* **1998**, *817*, 153–161.
(49) Adams, K. L.; Klunder, G. L.; Demas, V.; Malba, V.; Bernhardt, A.; Evans, L.; Harvey, C.; Maxwell, R. S.; Herberg, J. L. *Diffus. Fundam.* **2009**, *10*, 6.1–6.4.
(50) Malba, V.; Maxwell, R. S.; Evans, L.; Bernhardt, A.; Cosman, M.; Yan, K. *Biomed. Microdevices* **2003**, 21–27.
(51) Landers, J. P. *Handbook of Capillary Electrophoresis*, 2nd ed.; CRC Press: Boca Raton, FL, 1997.
(52) Krojanski, H. G.; Lambert, J.; Gerikalan, Y.; Suter, D.; Hergenröder, R. *Anal. Chem.* **2008**, *80*, 8668–8672.